A model for the high-energy emission of Cyg X-1

Igor V. Moskalenko[†⋆], Werner Collmar[†], Volker Schönfelder[†]

[†] *Max-Planck-Institut für extraterrestrische Physik, D-85740 Garching, Germany*
[⋆] *Institute for Nuclear Physics, Moscow State University, 119 899 Moscow, Russia*

Abstract. We construct a model of Cyg X-1 which describes self-consistently its emission from soft X-rays to MeV γ-rays. Instead of a compact pair-dominated γ-ray emitting region, we consider a hot optically thin and spatially extended proton-dominated cloud surrounding the whole accretion disc. The γ-ray emission is due to bremsstrahlung, Comptonization, and positron annihilation, while the corona-disc model is retained for the X-ray emission. We show that the Cyg X-1 spectrum accumulated by OSSE, BATSE, and COMPTEL in 1991–95, as well as the HEAO-3 γ_1 and γ_2 spectra can be well fitted by our model (see [1] for details). The derived parameters are in qualitative agreement with the picture in which the spectral changes are governed by the mass flow rate in the accretion disc. In this context, the hot outer corona could be treated as the advection-dominated flow co-existing with a standard thin accretion disc.

INTRODUCTION

Cyg X-1 is believed to be powered by accretion through an accretion disc. Its X-ray spectrum indicates the existence of a hot X-ray emitting and a cold reflecting gas. The soft blackbody component is thought to be thermal emission from an optically thick and cool accretion disc [2,3]. The hard X-ray part $\gtrsim 10$ keV with a break at ~ 150 keV has been attributed to thermal disc emission Comptonized by a corona with a temperature of ~ 100 keV [4,5]. A broad hump peaking at ~ 20 keV [6], an iron Kα emission line at ~ 6.2 keV [7], and a strong iron K-edge [8,9] have been interpreted as signatures of Compton reflection of hard X-rays off cold accreting material. There have also been reports of a hard component extending into the MeV region. Most famous was the so-called 'MeV bump' observed at a 5σ level during the HEAO-3 mission [10]. For a discussion of the pre-CGRO data see [11].

The average X-ray flux of Cyg X-1 shows a two-modal behavior. Most of its time it spends in a so-called 'low' state where the soft X-ray luminosity is low. There are occasional periods of 'high' state emission. Remarkable is

TABLE 1. Luminosity of Cyg X-1.

Energy band	Luminosity, 10^{36} erg/s
≥ 0.02 MeV	26
0.02–0.2 MeV	20.5
0.2–1 MeV	4.8
≥ 1 MeV	0.6

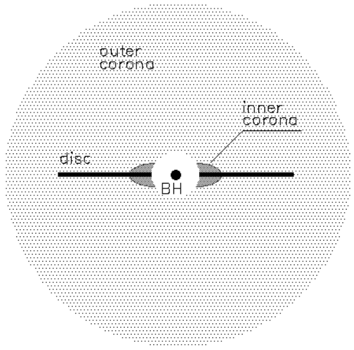

FIGURE 1. A schematic view.

the anticorrelation between the soft and hard X-ray components [5], which is clearly seen during transitions between the two states.

Since its launch in 1991 CGRO has observed Cyg X-1 several times. The COMPTEL spectrum shows significant emission out to several MeV, which however, remained always more than an order of magnitude below the MeV bump reported by HEAO-3. The spectrum accumulated between '91 and '95 by the COMPTEL [12], BATSE [13], and OSSE [14] instruments is shown in Fig. 2. Although the OSSE and BATSE normalizations are different, the spectral shape is very similar. Table 1 shows the average luminosity of Cyg X-1 (at 2.5 kpc) as derived from the BATSE-COMPTEL spectrum.

THE MODEL

The existence of a compact pair-dominated core around a BH in Cyg X-1 is probably ruled out by the CGRO observations. A signature of such a core would be a bump [15,16] similar to the one reported by HEAO-3. However no evidence for such a bump was found in the CGRO data [12,14]. Additionally, the luminosity of Cyg X-1 above 0.5 MeV, though small, exceeds substantially the Eddington luminosity for pairs, which is ~ 2000 times lower than for a hydrogen plasma. Also the hard MeV tail can not be explained by Comptonization in a corona ($kT \sim 100$ keV) and thus another mechanism is required.

We consider the proton-dominated optically thin solution [17], $\Theta \equiv \frac{kT}{m_e c^2} \lesssim 1$, where the γ-ray emission is attributed to a spatially extended cloud surrounding the whole accretion disc (Fig. 1), the outer corona, which emits via bremsstrahlung, Comptonization, and positron annihilation, and analyze possible consequences of that. We adopt a standard model for X-rays, where the hard X-rays are produced by Comptonization of the soft X-ray emission in an inner corona, and the soft X-rays are a composition of the local blackbody emission from the disc and the reflection component. The optical depth of the outer corona has to be so small that the disc and inner corona emission is only slightly reprocessed in it.

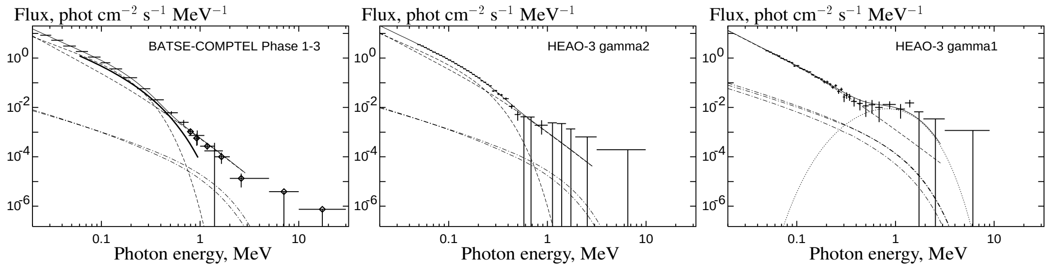

FIGURE 2. *Left panel:* the Cyg X-1 spectrum based on the CGRO Phase 1–3 observations (◇: the COMPTEL data [12], +: the BATSE data [13]). The thick solid line is the best fit to the time average OSSE spectrum [14]. *Central and right panels:* the HEAO-3 γ_2, γ_1 spectra [10]. In all panels the thin solid lines represent our model fit for the parameter sets I. The spectral components shown are the annihilation line (dotted line), *ee*-, e^+e^--, *ep*-bremsstrahlung (dash-dot), dashed lines: the Comptonized spectra from the *i*- and *o*-corona (shown up to 3 MeV, where it agrees with simulations, and also significant data points are available).

The spectral modelling has been carried out with the *ee*- and e^+e^--bremsstrahlung emissivities given by numerical fits of [18,19]. For the *ep*-bremssrahlung and annihilation emissivities we use the integration formulas of [18,20]. To calculate the effect of Compton scattering we follow the model of [21], which generally agrees well with Monte Carlo simulations except at high temperatures, $\Theta \sim 1$, and small optical depth. But it still provides a correct spectral index. We found that a power-law with a cutoff, $\propto \left[\frac{E_0}{E}\right]^{\alpha+1}(1-e^{-kT/E})$, where α is determined by the equation of [22], gives a reasonable agreement with Monte Carlo simulations up to ~ 3 MeV. The chosen normalization provides a correct value of the amplification factor [23]. The emission of the accretion disc which is reprocessed by the inner corona was taken monoenergetic, $E_0 = 1.6kT_{bb}$, where $kT_{bb} \approx 0.13$ keV is the effective temperature of the soft excess [3]. The intensity of the narrow annihilation line from the disc plane can be estimated by $I_a \simeq \frac{n_+ c}{4}\frac{R_d^2}{D^2}\cos i_d$, where n_+ is the e^+ number density in the outer corona, c the speed of light, R_d the disc radius, D the distance, and i_d ($\approx 40°$) the inclination angle of the disc plane.

The fitting parameters are: kT_i, τ_i, and kT_o, τ_o, the temperature and optical depth of the inner (i) and outer (o) coronae (spheres), $L^*_{\rm soft}$, the luminosity of the *disc* effectively Comptonized by the *i*-corona, $L_{\rm soft}$, the *total* effective luminosity of the central source in soft X-rays illuminating the *o*-corona, R, the *o*-corona radius, and, $Z = n_+/n_p$, the positron-to-proton ratio in it.

The bremsstrahlung and annihilation photon fluxes from the outer corona are proportional to $R^3 n_p^2$. Thus, if the annihilation contributes significantly, there is a continuum of solutions given by an equation $R^3 n_p^2 Z(1+Z) = \frac{R\tau_o^2 Z(1+Z)}{\sigma_T^2(1+2Z)^2} = const$, at kT_o, τ_o fixed, where $\frac{Z(1+Z)}{(1+2Z)^2}$ varies slowly for $Z \gtrsim 0.5$. For a negligible positron fraction the continuum of solutions is defined by $\tau_o = Rn_p\sigma_T = const$, where $R \le R_{\max}$, and $R_{\max}$ is fixed from fitting.

TABLE 2. The best fit model parameters.

Parameters	CGRO Phase 1–3		HEAO-3: γ_2-state		γ_1-state	
	I	II	I	II	I[a]	II
Soft X-ray luminosity, $L_{\rm soft}$ (10^{36} erg s^{-1})	9.7	10.6	10.6	10.7	9.8	7.9
i-corona temperature, kT_i (keV)	75.9	73.9	95	94.9	–	93.0
i-corona optical depth, τ_i	2.30	2.40	1.41	1.42	–	1.44
$L^*_{\rm soft}$, 10^{36} erg s^{-1}	0.86	0.83	1.96	1.95	–	0.51
o-corona temperature, kT_o (keV)	430	479	450	448	346	361
o-corona optical depth, τ_o	0.05	0.037	0.056	0.056	0.12	0.10
o-corona radius, R (10^8 cm)[b]	$\lesssim 100$	$\lesssim 100$	$\lesssim 100$	150	391	812
Positron-to-proton ratio, Z[b]	0	0	0	1.00	1.0	0.5
Proton number density, n_p (10^{10} cm^{-3})[b]	–	–	–	187	154	93
Accretion disc radius, R_d (10^8 cm)	–	–	–	1	1	1
I_a, 10^{-5} photons cm^{-2} s^{-1}	0	0	0	0.18	0.15	0.04
χ^2_ν	3.1	3.1	1.4	1.4	0.9	0.9

[a] The inner corona is small or even absent at all; [b] For R, n_p, Z dependence see text.

RESULTS AND DISCUSSION

The observed spectra of Cyg X-1 are shown in Fig. 2 together with our model calculations. The parameters obtained from spectral fitting are listed in Table 2. For comparison two parameter sets with the same χ^2_ν are shown, however the first one (I) seems to be more physical.

The average BATSE-COMPTEL spectrum corresponds probably to the normal state of Cyg X-1. Only two components contribute: the Comptonized emission from the inner and outer coronae. The parameters obtained for the HEAO-3 γ_2 state are similar, though the upper limits at $E_\gamma \gtrsim 1$ MeV allow some positron fraction (II). For the HEAO-3 γ_1 'bump' spectrum the outer corona size is several times larger, while the inner corona is small or even absent at all (set I). The non-negligible positron fraction (for R, n_p, Z dependence see above) is too high to be produced in the optically thin outer corona [17]. Therefore, we suggest a positron production mechanism, which could sometimes operate in the inner disc. The radiation pressure would necessarily cause a pair wind, which serves as energy input into the o-corona thereby increasing its radius.

The small luminosity of the disc which is Comptonized by the inner corona, $L^*_{\rm soft} \approx 10^{36}$ erg/s, probably implies a geometry where only the inner part of the disc is effectively covered by the corona. Otherwise, if the corona forms a disc-like structure where the intensity depends on the inclination angle, then it should cover almost all of the X-ray emitting area of the disc.

The soft (< 10 keV) X-ray luminosity of Cyg X-1 is $\sim 8.5 \times 10^{36}$ erg/s on average [5], while during the HEAO-3 γ_1, γ_2 states it was even lower [10]. Taking into account that for hard X-ray photons the Comptonization efficiency in the hot plasma drops substantially [21] while the number of photons decreases as well, the obtained values, $L_{\rm soft} \approx 10^{37}$ erg/s, match the data.

No pairs are required to reproduce the spectrum of Cyg X-1 in its normal state. If one takes $I_a \approx 4.4 \times 10^{-4}$ photons cm^{-2} s^{-1} [24] for the annihilation line flux in the γ_1 state, it allows the accretion disc radius to be estimated to $R_d \sim 1.7 \times 10^9$ cm (set I). The allowed upper limit derived from optical measurements is $R_d \approx 6 \times 10^9$ cm $(M/10M_\odot)$ [5].

The obtained parameters are consistent with a picture where the spectral changes are governed by the mass accretion rate $\dot{M}$ [25]. The γ_1 state probably corresponds to a smaller $\dot{M}$ compared to the normal state. In this context, the γ-ray luminosity should anticorrelate with the hard X-ray luminosity. The extended hot outer corona can be treated as the advection-dominated accretion flow (ADAF) co-existing with a cool optically thick disc, though in contrast to a standard ADAF [25], the electrons here are hot and the protons are cold. This is possible since cooling via bremsstrahlung and Coulomb *ep*-collisions at low density is unimportant while small optical depth prevents from effective Compton cooling. The adequate heating could be provided by the electron thermal conduction from a region with nearly virial ion temperature.

Useful discussions with N.Shakura, R.Narayan, L.Titarchuk, and M.Gilfanov are greatly acknowledged. We are particularly grateful to M.McConnell for providing us with the combined spectra of Cyg X-1 prior to publication, and E.Churazov for Monte Carlo simulations of Comptonization in $\Theta \sim 1$, $\tau \approx 0.1 - 0.05$ plasma.

REFERENCES

1. Moskalenko I. V., Collmar W., Schönfelder V., in preparation (1997)
2. Pringle J. E., *ARA&A* **19**, 137 (1981)
3. Bałucińska-Church M., et al., *A&A* **302**, L5 (1995)
4. Sunyaev R. A., Titarchuk L. G., *A&A* **86**, 121 (1980)
5. Liang E. P., Nolan P. L., *Spa. Sci. Rev.* **38**, 353 (1984)
6. Done C., et al., *ApJ* **395**, 275 (1992)
7. Barr P., White N., Page C. G., *MNRAS* **216**, 65p (1985)
8. Inoue H., in *Proc. 23rd ESLAB Symp.*, Noordwijk: ESA, 1989, **2**, p.783
9. Tanaka Y., *Lect. Notes in Phys.* **385**, 98 (1991)
10. Ling J. C., et al., *ApJ* **321**, L117 (1987)
11. Owens A., McConnell M. L., *Comments Astrophys.* **16**, 205 (1992)
12. McConnell M., et al., in *AIP Proc.*, 1997, this Symposium
13. Ling J. C., et al., *ApJS*, submitted (1997)
14. Phlips B. F., et al., *ApJ* **465**, 907 (1996)
15. Liang E. P., Dermer C. D., *ApJ* **325**, L39 (1988)
16. Liang E. P., *A&A* **227**, 447 (1990)
17. Svensson R., *MNRAS* **209**, 175 (1984)
18. Stepney S., Guilbert P. W., *MNRAS* **204**, 1269 (1983)
19. Haug E., *A&A* **178**, 292 (1987)
20. Dermer C. D., *ApJ* **280**, 328 (1984)
21. Hua X.-M., Titarchuk L., *ApJ* **449**, 188 (1995)
22. Titarchuk L., Lyubarskij Yu., *ApJ* **450**, 876 (1995)
23. Dermer C. D., Liang E. P., Canfield E., *ApJ* **369**, 410 (1991)
24. Ling J. C., Wheaton Wm. A., *ApJ* **343**, L57 (1989)
25. Narayan R., *ApJ* **462**, 136 (1996)